

Superintense highly anisotropic optical transitions in anisotropic quantum dots

Siranush Avetisyan,¹ Pekka Pietiläinen,² and Tapash Chakraborty^{1,*}

¹*Department of Physics and Astronomy, University of Manitoba, Winnipeg, Manitoba, Canada R3T 2N2*

²*Department of Physics/Theoretical Physics, University of Oulu, Oulu FIN-90014, Finland*

(Received 20 August 2013; published 22 November 2013)

Coulomb interaction among electrons is found to have profound effects on the electronic properties of anisotropic quantum dots in a perpendicular external magnetic field and in the presence of the Rashba spin-orbit interaction. This is more evident in optical transitions, which we find in this system to be highly anisotropic and superintense, in particular, for large values of the anisotropy parameter.

DOI: [10.1103/PhysRevB.88.205310](https://doi.org/10.1103/PhysRevB.88.205310)

PACS number(s): 73.21.La, 78.67.Hc

I. INTRODUCTION

For more than two decades, theoretical studies of quantum dots (QDs) in an external magnetic field¹ have largely focused on the properties of dots with circular symmetry.^{2,3} Extensive investigations of transport and optical spectroscopy of these semiconductor nanostructures (the *artificial atoms*) have revealed several important atomic-like properties.^{2,3} In contrast, not enough is known about the electronic properties of anisotropic quantum dots.^{4,5} Another important direction of the QD research that is gaining popularity in recent years has been the role of Rashba spin-orbit interaction (SOI)^{6–8} in quantum dots. The importance of this interaction in semiconductor spintronics has been well documented in the literature.^{9–11} Detailed theoretical studies of the influence of Rashba SOI on the electronic properties of QDs with isotropic confinement have already been reported earlier,¹² where the SO coupling was found to manifest itself mainly in multiple level crossings and level repulsions in the energy spectra. These were attributed to an interplay between the Zeeman effect and the SOI present in the system Hamiltonian. Those effects, in particular the level repulsions, were weak and as a result, would require extraordinary efforts to detect the strength of SO coupling¹³ in those systems. On the other hand, by introducing anisotropy in a QD, we have previously shown that a major enhancement of the Rashba SO coupling effects can be achieved in the Fock-Darwin spectra.¹⁴ Although various approximate schemes exist to study the effects of anisotropy on the far-infrared absorption,¹⁵ the role of SO coupling on the far-infrared response,¹⁶ or other physical properties of elliptical dots,¹⁷ an accurate and coherent theoretical treatment of all these issues, in particular, the role of Coulomb interaction, in conjunction with all these properties is seriously lacking. Here we demonstrate that in the presence of the Coulomb interaction among the electrons, and combined with the Rashba SOI, the eccentricity of the QD is responsible for major modification of the electron energy spectra, which clearly manifests itself in superintense and highly anisotropic optical transitions that are vastly different from those that are commonly observed in an isotropic QD.

II. THEORETICAL MODEL

Until now, interacting electrons in elliptical QDs have been studied by means of perturbative approaches.^{18,19} In what follows, we present a nonperturbative, exact

diagonalization scheme to treat interacting electrons in anisotropic quantum dots. Our complete single-particle Hamiltonian of an electron moving in the xy plane and subjected to an external perpendicular magnetic field with the vector potential $\mathbf{A} = \frac{1}{2}B(-y, x)$ is

$$\mathcal{H} = \frac{1}{2m_e} \left(\mathbf{p} - \frac{e}{c} \mathbf{A} \right)^2 + \frac{1}{2} m_e (\omega_x^2 x^2 + \omega_y^2 y^2) + \frac{\alpha}{\hbar} \left[\boldsymbol{\sigma} \times \left(\mathbf{p} - \frac{e}{c} \mathbf{A} \right) \right]_z + \frac{1}{2} g \mu_B B \sigma_z.$$

The first two terms on the right-hand side describe a two-dimensional harmonic oscillator confined by an elliptic potential.⁴ The next term takes care of the SOI while the last one is for the Zeeman coupling. In order to treat the Coulomb interaction we rearrange the terms in the Hamiltonian into three parts:

$$\mathcal{H}_\Lambda = \frac{1}{2m_e} (p_x^2 + p_y^2 + \Omega_x^2 x^2 + \Omega_y^2 y^2), \quad \mathcal{H}_Z = \frac{1}{2} g \mu_B B \sigma_z, \\ \mathcal{H}_R = \frac{1}{2} \omega_c (y p_x - x p_y) + \frac{\alpha}{\hbar} \left[\sigma_x \left(p_y - \frac{e B_\perp}{2c} x \right) - \sigma_y \left(p_x + \frac{e B_\perp}{2c} y \right) \right],$$

where \mathcal{H}_Λ describes a two-dimensional spinless harmonic oscillator, the Zeeman coupling \mathcal{H}_Z introduces the spin, and \mathcal{H}_R deforms the simple Cartesian phase space of the operators \mathcal{H}_Λ and \mathcal{H}_Z . We have also introduced the cyclotron frequency $\omega_c = eB/m_e c$ and the oscillator frequencies $\Omega_{x,y}^2 = m_e^2 (\omega_{x,y}^2 + \frac{1}{4} \omega_c^2)$. The eigenstates $|\lambda\rangle$ of the oscillator Hamiltonian \mathcal{H}_Λ are just direct products $|n_x^\lambda\rangle |n_y^\lambda\rangle$ of the two harmonic oscillator states represented by the quantum numbers $n_{x,y}^\lambda$. Inclusion of the Zeeman term is also straightforward: we multiply the states $|\lambda\rangle$ with the eigenstates $|s_z\rangle$ of the Pauli spin matrix σ_z yielding the states $|\xi\rangle = |\lambda^\xi\rangle |s_z^\xi\rangle$. Finally, the effects of the operator \mathcal{H}_R are incorporated by diagonalizing it in the base spanned by the eigenstates $|\xi\rangle$ of the combination $\mathcal{H}_\Lambda + \mathcal{H}_Z$. Thus the eigenstates $|\gamma\rangle$ of the total single-electron Hamiltonian \mathcal{H} are expressed as superpositions of the states $|\xi\rangle$.

To handle the mutual interactions between electrons, we work in the occupation number representation based on the eigenstates of the Hamiltonian \mathcal{H} . Then the main task is to

evaluate the two-body matrix elements

$$\begin{aligned} \langle \gamma_1 \gamma_2 | V | \gamma_3 \gamma_4 \rangle &= \int d\mathbf{x}_1 d\mathbf{x}_2 \Phi_{\gamma_1}^*(\mathbf{x}_1) \Phi_{\gamma_2}^*(\mathbf{x}_2) \\ &\quad \times V(|\mathbf{x}_1 - \mathbf{x}_2|) \Phi_{\gamma_3}(\mathbf{x}_2) \Phi_{\gamma_4}(\mathbf{x}_1), \end{aligned}$$

where the wave functions $\Phi_\gamma(\mathbf{x})$ correspond to the eigenstates $|\gamma\rangle$ of \mathcal{H} and the integrals over the variables \mathbf{x} include also summation over the spin degrees of freedom. The expansion of the functions Φ_γ in terms of the wave functions corresponding to the eigenstates $|\xi\rangle$ of $\mathcal{H}_\Lambda + \mathcal{H}_Z$ leads to evaluations of two-body matrix elements between the states $|\xi\rangle$. Since the electrons act via the Coulomb potential $V(|\mathbf{x}|) = V_C(r) = e^2/\epsilon r$, where ϵ is the background dielectric constant, the summations over spin degrees of freedom yield only Kronecker deltas of the s_z quantum numbers and we are left with the matrix elements

$$\begin{aligned} \langle \lambda_1 \lambda_2 | V | \lambda_3 \lambda_4 \rangle &= \int d\mathbf{r}_1 d\mathbf{r}_2 \psi_{\lambda_1}^*(\mathbf{r}_1) \psi_{\lambda_2}^*(\mathbf{r}_2) \\ &\quad \times V(|\mathbf{r}_1 - \mathbf{r}_2|) \psi_{\lambda_3}(\mathbf{r}_2) \psi_{\lambda_4}(\mathbf{r}_1) \end{aligned}$$

between pairs of the single-particle oscillator wave functions. In isotropic parabolic dots with mutual Coulomb interactions we could use the explicit algebraic formula,¹² but in elliptical confinements we have to resort to numerical computations. Perhaps the most cost-effective way is to do the evaluation via the (two-dimensional) Fourier transforms

$$\begin{aligned} \tilde{\Psi}_{\mu\nu}(\mathbf{k}) &= \int d\mathbf{r} e^{i\mathbf{k}\cdot\mathbf{r}} \psi_\mu^*(\mathbf{r}) \psi_\nu(\mathbf{r}), \\ \tilde{V}(\mathbf{k}) &= \int d\mathbf{r} e^{i\mathbf{k}\cdot\mathbf{r}} V(\mathbf{r}) \end{aligned}$$

of the products of the wave functions and the interaction. A straightforward algebra yields the expression

$$\langle \lambda_1 \lambda_2 | V | \lambda_3 \lambda_4 \rangle = \frac{1}{(2\pi)^2} \int d\mathbf{k} \tilde{\Psi}_{\lambda_4 \lambda_1}^*(\mathbf{k}) \tilde{\Psi}_{\lambda_2 \lambda_3}(\mathbf{k}) \tilde{V}(\mathbf{k}).$$

Numerical computation of this final twofold integral is a relatively fast operation.

Since for the Coulomb interactions we know the Fourier transform to be $\tilde{V}_C(\mathbf{k}) \propto 2\pi e^2/k$, we are left with the evaluation of the Fourier transforms $\tilde{\Psi}_{\mu\nu}(\mathbf{k})$. We have experimented with two practically equally efficient methods: the first one is fully generic and applicable to any system while the second one is restricted to elliptical confinements. The generic method is based on the observation that the Fourier transform $\tilde{\Psi}_{\mu\nu}(\mathbf{k})$ can in fact be written as the matrix element of the exponential of the position operator \mathbf{r}_{op} , $\tilde{\Psi}_{\mu\nu}(\mathbf{k}) = \langle \mu | e^{i\mathbf{k}\cdot\mathbf{r}_{\text{op}}} | \nu \rangle$. Since the components x_{op} and y_{op} of the position operator commute we actually need the matrix elements of the exponential operators $\exp(ix_{\text{op}})$ and $\exp(iy_{\text{op}})$. These in turn are easily evaluated by diagonalizing the matrix X with matrix elements $X_{\mu\nu} = \langle \mu | x_{\text{op}} | \nu \rangle$ and applying the inverse unitary transformation taking X to the diagonal form to the exponentiated diagonal, together with the similar procedure for the operator y_{op} .

In the second approach we take advantage of the fact that the single-particle wave functions are products of two Hermite functions, one with the x coordinate and the other with the y coordinate as the argument. This implies that the product $\psi_\mu^*(\mathbf{r}) \psi_\nu(\mathbf{r})$ to be transformed factorizes to a product of two

functions depending on x and y , respectively. In fact we can do the resulting one-dimensional transforms yielding

$$\tilde{\Psi}_{\mu\nu}(\mathbf{k}) = \tilde{\mathcal{G}}_{n_x^\mu, n_x^\nu}^x(k_x) \tilde{\mathcal{G}}_{n_y^\mu, n_y^\nu}^y(k_y),$$

where the functions $\tilde{\mathcal{G}}_{i,j}^{x,y}(k)$ are given by

$$\begin{aligned} \tilde{\mathcal{G}}_{ij}^{x,y}(k) &= (-1)^m \sqrt{\frac{n!}{(n+\xi)!}} (\beta_{x,y} k)^\xi e^{-\frac{1}{2}(\beta_{x,y} k)^2} \\ &\quad \times L_n^\xi((\beta_{x,y} k)^2) (\delta_{p,0} + i\delta_{p,1}). \end{aligned}$$

In the above formulas the symbols $n_{x,y}^\mu$ and $n_{x,y}^\nu$ stand for the x and y oscillator quantum numbers of the states labeled by μ and ν . We have also introduced the shorthand notations $\beta_{x,y} = \sqrt{\frac{\hbar}{2m_e\omega_{x,y}}}$, $n = \min(i, j)$, $\xi = |i - j|$, $p = \xi \bmod 2$. Although both approaches introduced here have their merits, it should be noted that the first method is somewhat more general and applicable to any system, while the second method works only for the harmonic oscillator basis. The second method is however computationally slightly faster than the first.

III. RESULTS AND DISCUSSION

In our numerical studies that follow, we have used the parameters corresponding to the InAs QD,¹⁴ where strong SOI was reported experimentally.¹¹ The results for the energy spectra are displayed in Figs. 1–3 for various values of the SO coupling strength α and the anisotropy. In the absence of the external magnetic field and the SOI, neither the total spin S nor its z -component S_z appear in the *full* Hamiltonian (with Coulomb interactions). We therefore expect the two-electron systems to consist of $S = 0$ spin singlets and $S = 1$ spin triplets. The energy spectra of Fig. 1 indeed confirm that to be the case: the dispersions form bunches of one and three lines, the latter of which diverges due to the Zeeman splitting when the magnetic field increases. Perhaps the most noticeable feature shown in Fig. 1 is the singlet-triplet transition of the

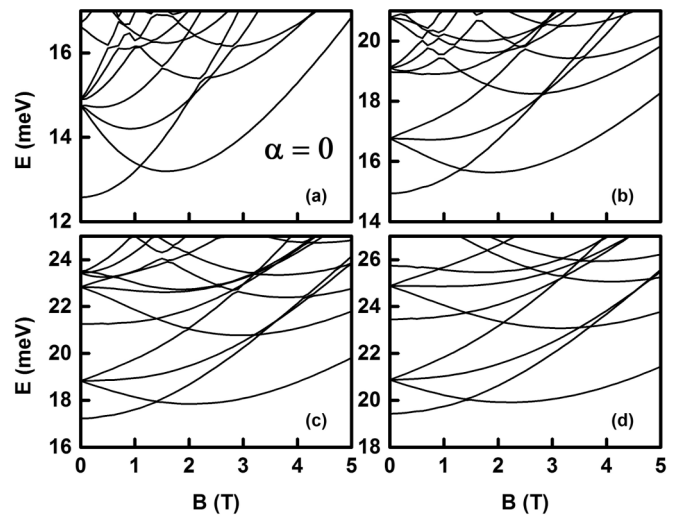
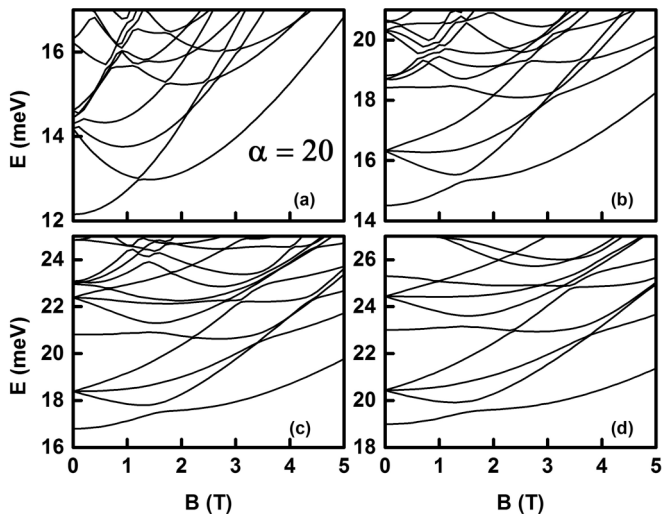


FIG. 1. Magnetic field dependence of the low-lying two-electron energy levels of an elliptical dot without the Rashba SOI ($\alpha = 0$). The results are for $\omega_x = 4$ meV and (a) $\omega_y = 4.1$ meV, (b) $\omega_y = 6$ meV, (c) $\omega_y = 8$ meV, and (d) $\omega_y = 10$ meV.

FIG. 2. Same as in Fig. 1, but for $\alpha = 20$ meV nm.

ground state for magnetic fields slightly above 1 T. The origin of this crossing of the dispersion lines can be traced to the crossing of the second and third lowest energy levels of the single-electron systems.¹⁴

Just as for the circular QD, the spin singlet-triplet transition (at $B \simeq 1.5$ T in Fig. 1) is the only transition in the ground state. The critical field where the transition takes place is somewhat dependent on the method of calculation and the choice of material parameters.¹⁸ The main role of the Coulomb interaction is the upward shift of the spectral lines and lifting of the accidental degeneracies. Surprisingly, the interaction also practically freezes the movement of the singlet-triplet transition point to higher fields when the eccentricity increases. In the absence of the electron-electron interaction the transition point shifts about 2 T whereas in the presence of the interactions the shift is only few tenths of a tesla with the same eccentricities. When the SOI is turned on (Fig. 2 and Fig. 3) most of the characteristic features of Fig. 1 survive. However, since the SOI can mix spin-up and spin-down single-particle states, neither S nor S_z are any longer good quantum numbers. This is clearly evident in the singlet-triplet transition which

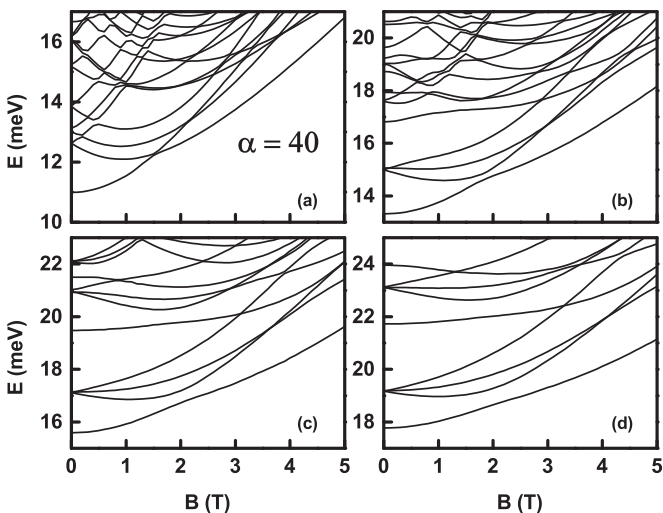
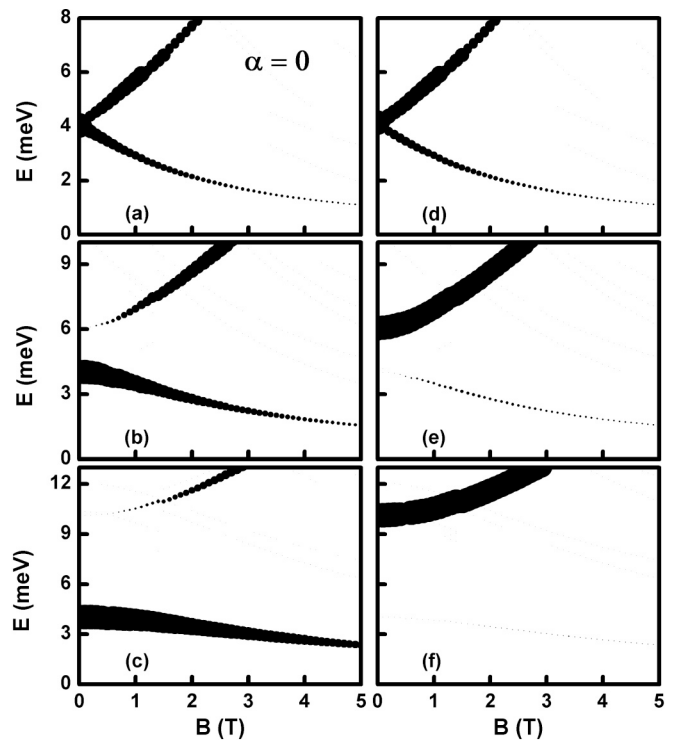
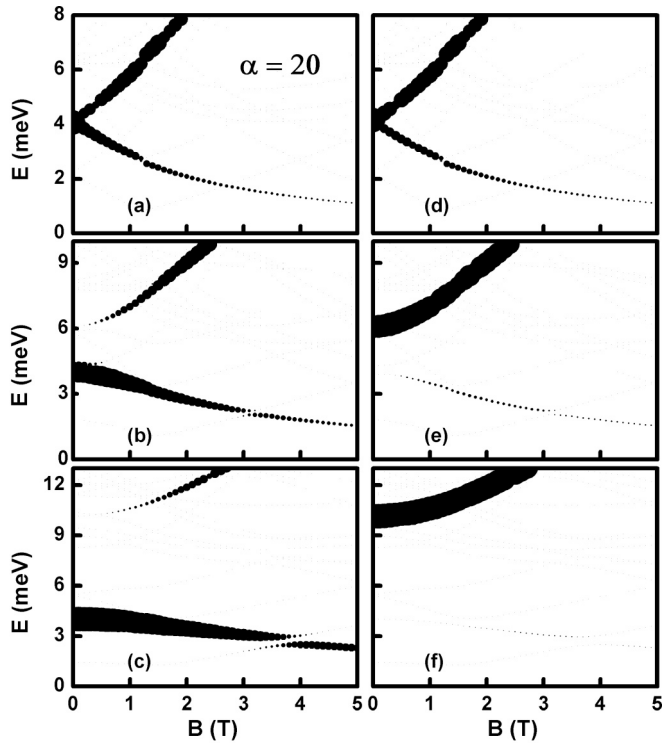
FIG. 3. Same as in Fig. 1, but for $\alpha = 40$ meV nm.

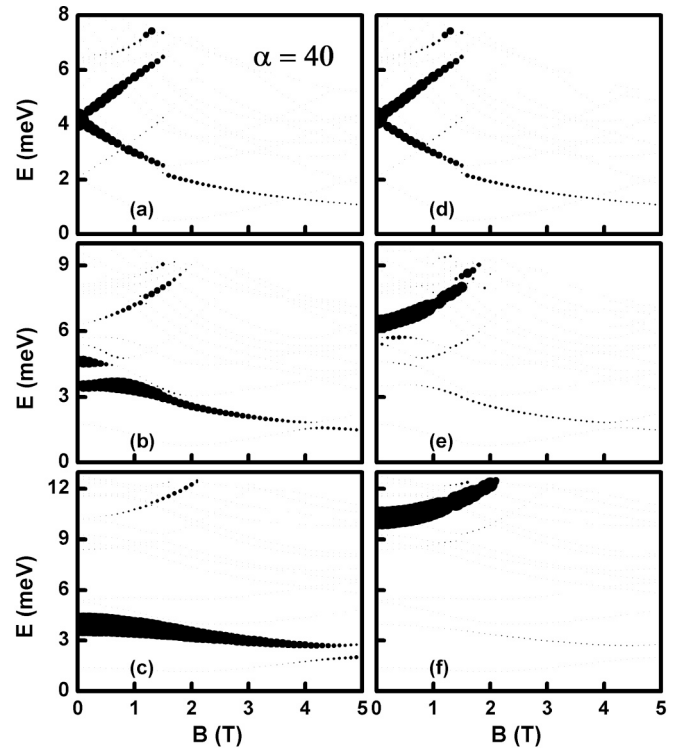
FIG. 4. Optical absorption (dipole allowed) spectra of elliptical QDs with $\alpha = 0$ meV nm for various choice of anisotropy parameters: (a) $\omega_x = 4$ meV, $\omega_y = 4.1$, (b) $\omega_x = 4$ meV, $\omega_y = 6$ meV, and (c) $\omega_x = 4$, $\omega_y = 10$. The polarization of the incident radiation is along the x axis. The parameters for (d)–(f) are the same, except that the incident radiation is polarized along the y axis. The areas of the filled circles are proportional to the calculated absorption cross section.

transforms to anticrossing in the presence of the SOI. Several similar kind of crossing-anticrossing conversions can also be seen higher in the spectra.

In Figs. 4–6 we show the the absorption cross sections for the dipole allowed transitions¹⁴ from the ground states corresponding to the energy spectra of Figs. 1–3. To evaluate the cross sections we express the dipole operator in the occupation representation as the single-particle operator $P = \sum_{ij} \langle \gamma_i | \epsilon \cdot \mathbf{r} | \gamma_j \rangle a_i^\dagger a_j$, where ϵ is the polarization of the incident radiation and the operators a^\dagger (a) create (destroy) the single-particle SOI states $|\gamma\rangle$. Computation of the matrix element of this polarization operator between ground state and the excited states of the full Hamiltonian (mutual Coulomb interactions included) yields transition amplitudes for the absorption. We explore the cases where the incident radiation is polarized along the x and y directions. Although the energy conservation forces the absorbed energies to match the transition energies the dipole absorptions are mostly probing the single-particle properties of the dot. This is clear from the explicit expression of the dipole operator P : the radiation can affect only one electron at a time by kicking it to a higher unoccupied selection rule allowed state. In particular, chosen polarizations explore the oscillator strengths along the x and y directions. Consequently we expect the absorption spectra to resemble approximately the spectra of


 FIG. 5. Same as in Fig. 4, but for $\alpha = 20$ meV nm.

the one-particle system. This indeed seems to be the case. Except for the case of almost isotropic QDs [panels (a) and (c)], the optical transitions are clearly highly anisotropic. For example, because the y -polarization probes for oscillations along the y direction the related transitions go mostly to the upper mode; i.e., the favored transition energies are 4, 6, and 10 meV in panels (d)–(f). The resulting transitions are therefore superintense, unlike in isotropic QDs. There are also weak-intensity transitions to the lower mode. This is due to the magnetic field and the SOI, both of which distort the confinement ellipsoid. There are of course some notable deviations from the single-electron case. For example, because the Coulomb interaction couples several noninteracting states there can be many more allowed transitions from a given interacting state than from a noninteracting one resulting in different absorption intensities. The second and perhaps the most notable example of the multiparticle nature of the system may be the reflection of the ground-state singlet-triplet anticrossings in the cross section.


 FIG. 6. Same as in Fig. 5, but for $\alpha = 40$ meV nm.

To summarize: we have reported here detailed and accurate studies of anisotropic quantum dots with interacting electrons in the presence of the Rashba SOI. The Coulomb interaction in the presence of the spin-orbit coupling exhibits a very strong effect, particularly in the presence of strong anisotropy. This is clearly seen in the optical absorption spectra which is superintense and highly anisotropic. The spectra derived here are entirely different from the ones observed thus far in isotropic QDs. Our present work can be generalized, in a straightforward manner, to include more interacting electrons in the QD. The energy spectra and optical transitions with more electrons will undoubtedly be very complex. However, the basic properties uncovered here will remain intact.

ACKNOWLEDGMENTS

The work was supported by the Canada Research Chairs Program of the Government of Canada.

*tapash.chakraborty@umanitoba.ca

¹P. A. Maksym and T. Chakraborty, *Phys. Rev. Lett.* **65**, 108 (1990).

²T. Chakraborty, *Quantum Dots* (North-Holland, Amsterdam, 1999).

³D. Heitmann, editor, *Quantum Materials* (Springer, Heidelberg, 2010).

⁴A. V. Madhav and T. Chakraborty, *Phys. Rev. B* **49**, 8163 (1994).

⁵A. Singha, V. Pellegrini, S. Kalliakos, B. Karmakar, A. Pinczuk, L. N. Pfeiffer, and K. W. West, *Appl. Phys. Lett.* **94**, 073114 (2009);

M. Hochgräfe, Ch. Heyn, and D. Heitmann, *Phys. Rev. B* **63**, 035303 (2000); D. G. Austing, S. Sasaki, S. Tarucha, S. M. Reimann, M. Koskinen, and M. Manninen, *ibid.* **60**, 11514 (1999).

⁶Y. A. Bychkov and E. I. Rashba, *J. Phys. C* **17**, 6039 (1984).

⁷H.-A. Engel, B. I. Halperin, and E. I. Rashba, *Phys. Rev. Lett.* **95**, 166605 (2005).

⁸In InAs quantum well structures, the Dresselhaus SOI is quite appreciable, but the Rashba contribution is still dominant; see, e.g., S. Giglberger *et al.*, *Phys. Rev. B* **75**, 035327 (2007).

- ⁹For recent comprehensive reviews, see T. Dietl, D. D. Awschalom, M. Kaminska, and H. Ono, editors, *Spintronics* (Elsevier, Amsterdam, 2008); I. Žutić, J. Fabian, and S. Das Sarma, *Rev. Mod. Phys.* **76**, 323 (2004); J. Fabian, A. Matos-Abiague, C. Ertler, P. Stano, and I. Žutić, *Acta Phys. Slov.* **57**, 565 (2007); M. W. Wu, J. H. Jiang, and M. Q. Weng, *Phys. Rep.* **493**, 61 (2010).
- ¹⁰J. Nitta, T. Akazaki, H. Takayanagi, and T. Enoki, *Phys. Rev. Lett.* **78**, 1335 (1997); M. Studer, G. Salis, K. Ensslin, D. C. Driscoll, and A. C. Gossard, *ibid.* **103**, 027201 (2009); D. Grundler, *ibid.* **84**, 6074 (2000).
- ¹¹H. Sanada, T. Sogawa, H. Gotoh, K. Onomitsu, M. Kohda, J. Nitta, and P. V. Santos, *Phys. Rev. Lett.* **106**, 216602 (2011); S. Takahashi, R. S. Deacon, K. Yoshida, A. Oiwa, K. Shibata, K. Hirakawa, Y. Tokura, and S. Tarucha, *ibid.* **104**, 246801 (2010); Y. Igarashi, M. Jung, M. Yamamoto, A. Oiwa, T. Machida, K. Hirakawa, and S. Tarucha, *Phys. Rev. B* **76**, 081303(R) (2007).
- ¹²T. Chakraborty and P. Pietiläinen, *Phys. Rev. Lett.* **95**, 136603 (2005); P. Pietiläinen and T. Chakraborty, *Phys. Rev. B* **73**, 155315 (2006); T. Chakraborty and P. Pietiläinen, *ibid.* **71**, 113305 (2005); A. Manaselyan and T. Chakraborty, *Europhys. Lett.* **88**, 17003 (2009).
- ¹³H.-Y. Chen, V. Apalkov, and T. Chakraborty, *Phys. Rev. B* **75**, 193303 (2007).
- ¹⁴S. Avetisyan, P. Pietiläinen, and T. Chakraborty, *Phys. Rev. B* **85**, 153301 (2012); **86**, 239901(E) (2012).
- ¹⁵I. Magnusdottir and V. Gudmundsson, *Phys. Rev. B* **60**, 16591 (1999).
- ¹⁶L. Serra, M. Valin-Rodriguez, and A. Puente, *Surf. Sci.* **532–535**, 576 (2003).
- ¹⁷G. Rezaei, Z. Mousazadeh, and B. Vaseghi, *Physica E* **42**, 1477 (2010); L. Serra, A. Puente, and E. Lipparini, *Int. J. Quantum Chem.* **91**, 483 (2003); E. Lipparini, L. Serra, and A. Puente, *Eur. Phys. J. B* **27**, 409 (2002); M. van den Broek and F. M. Peeters, *Physica E* **11**, 345 (2001); I. Magnusdottir and V. Gudmundsson, *Phys. Rev. B* **61**, 10229 (2000).
- ¹⁸P. A. Maksym, *Physica B* **249–251**, 233 (1998); Y.-H. Liu, F.-H. Yang, and S. L. Feng, *J. Appl. Phys.* **101**, 063714 (2007).
- ¹⁹M. M. Glazov and V. D. Kulakovskii, *Phys. Rev. B* **79**, 195305 (2009); S. Grap, V. Meden, and S. Andergassen, *ibid.* **86**, 035143 (2012).